Anisotropic Vacancy Kinetics and Single-Domain Stabilization on Si(100)-2×1

P. Bedrossian[(a)] and T. Klitsner
Sandia National Laboratories, Albuquerque, New Mexico 87185
(Received 2 October 1991)

Preferential annihilation of mobile surface vacancies at the ends, rather than the sides of dimer rows leads to a new, nonequilibrium, single-domain phase of Si(100) that is not accessible by epitaxial growth but is stable at moderate temperatures ($T \sim 450$ °C). These results emerge from a tunneling microscope study of layer-by-layer removal of Si from Si(100) under 225-eV Xe-ion bombardment.

PACS numbers: 79.20.Rf, 61.16.Di, 68.35.Fx

Several recent experiments using diffraction oscillations [1,2] and tunneling microscopy (STM) [3,4] have established (i) that the evolution of both metal surfaces and Si under low-energy (< 250 eV) ion bombardment is mediated by mobile surface vacancies created during sputtering, and (ii) that aspects of surface evolution under low-energy sputtering can be described in terms analogous to those associated with epitaxial growth. Specifically, mobile surface vacancies can nucleate monolayer-deep depressions, or "vacancy islands," and can annihilate at step edges. An understanding of surface vacancy kinetics is therefore an important component of a general description of low-energy-ion/solid interactions, and in particular of the development of advanced growth techniques that employ ion-beam stimulation [5,6].

We analyze the kinetics of surface vacancies on silicon via the natural analogy with adatom kinetics in growth. Recent STM studies provide a quantitative description of the anisotropic adatom diffusion and accommodation in Si/Si(100) homoepitaxy [7,8]. In particular, they show that preferential incorporation of impinging atoms at the ends rather than the sides of dimer rows is responsible for the more rapid progression of the "ragged" (S_B) steps relative to the "straight" (S_A) steps and, consequently, the metastable enhancement of the domain (B) with dimer rows perpendicular to the step edges. (We employ Chadi's notation for step classification [9].)

Here we report the first demonstration of anisotropic, surface vacancy annihilation on Si(100), using STM to observe the relative retraction of straight and ragged steps on that surface following sputtering. We show that the formation of a new, single-A-domain Si(100) surface, which is stable at common growth temperatures ($T \sim 450$ °C), is a consequence of the anisotropy of vacancy annihilation at steps.

Si(100) wafers, offcut 0.2° toward the [110] direction as measured by x-ray diffraction, were initially cleaned chemically [10] and then transferred to an ultrahigh vacuum chamber, where 1.0-keV Xe sputtering followed by annealing at 1150 °C produced a strong 2×1 pattern in low-energy electron diffraction. As shown in Fig. 1, the misorientation results in roughly equally spaced terraces, separated by single atomic steps. The 90° relative orientation of dimer rows on adjacent terraces leads to alternating A and B domains; type A has dimer rows running parallel to the step edge, and type B consists of dimers that run perpendicular to the step edge.

A surface prepared in this manner was exposed to 225-eV Xe-ion bombardment at a flux of 0.33 μA/cm^2. Sample temperatures were calibrated with an infrared

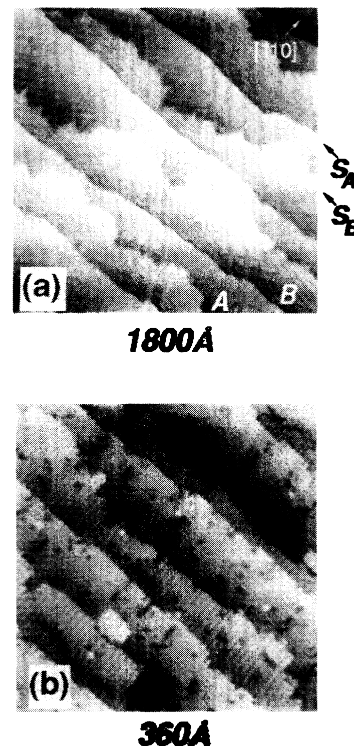

FIG. 1. (a) 1800-Å STM image of the 0.2°-offcut Si(100)-2×1 starting surface for subsequent sputtering. In this and subsequent images, the tunnel current is 0.8 nA and the tip bias +1.8 V, i.e., occupied sample states are imaged. The A and B terraces and the S_A and S_B steps are labeled. (b) Higher-resolution, 360-Å STM image of 1°-offcut Si(100)-2×1, showing the alternating dimer orientation on adjacent terraces. The more offcut sample is shown only in this figure in order to fit several terraces into a higher-resolution image.

 © 1992 The American Physical Society

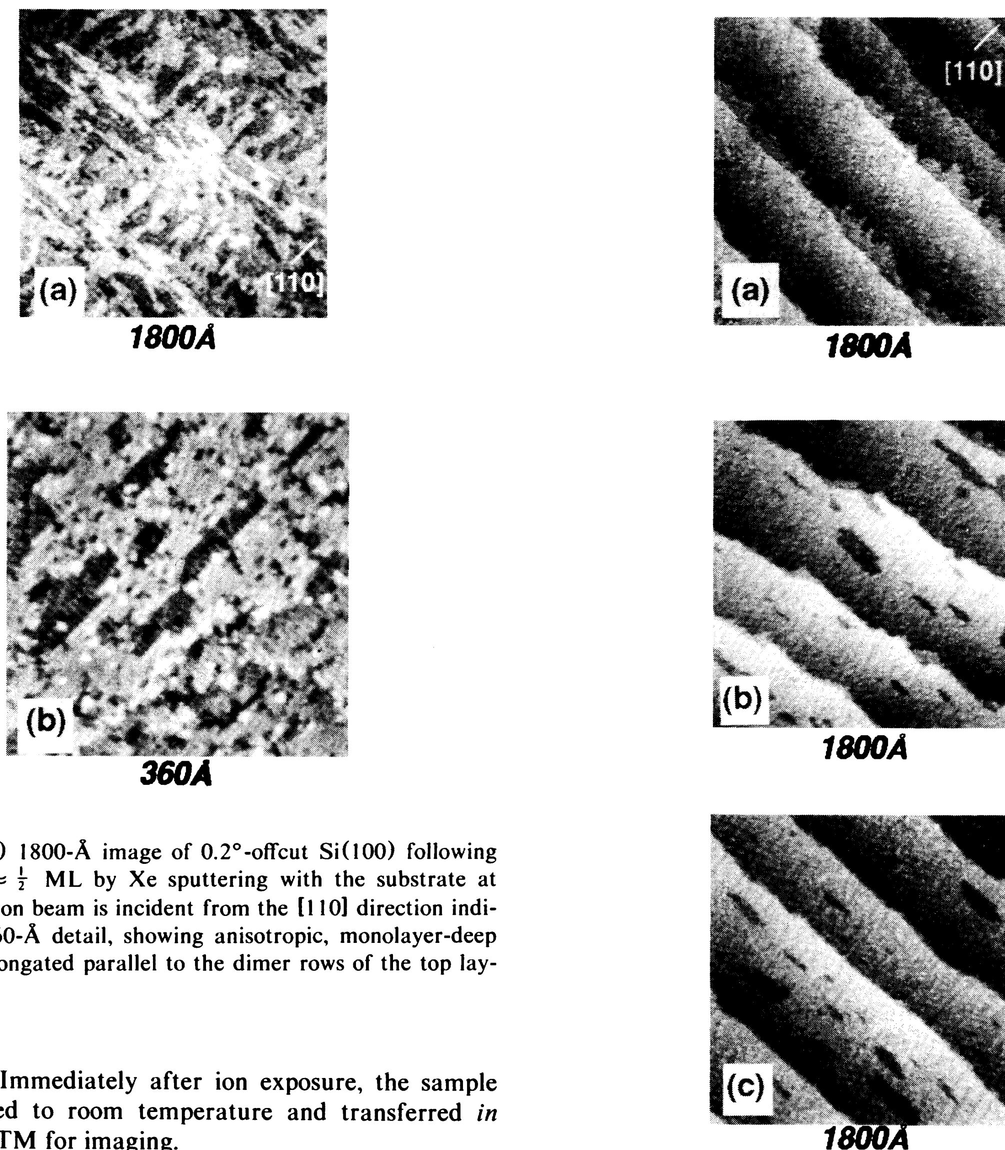

FIG. 2. (a) 1800-Å image of 0.2°-offcut Si(100) following removal of $\approx \frac{1}{2}$ ML by Xe sputtering with the substrate at 400 °C. The ion beam is incident from the [110] direction indicated. (b) 360-Å detail, showing anisotropic, monolayer-deep depressions elongated parallel to the dimer rows of the top layer.

FIG. 3. (a) 1800-Å image following Xe sputtering of $\approx \frac{1}{2}$ ML at 450 °C, showing depletion of the B domain. (b) 1800-Å image following Xe sputtering of ≈ 1 ML at 450 °C, showing further depletion of the B domain and nucleation of depressions in the A domain. (c) 1800-Å image following 6 min of annealing the surface shown in (b) at 450 °C. The B domain has virtually disappeared.

pyrometer. Immediately after ion exposure, the sample was quenched to room temperature and transferred *in situ* to the STM for imaging.

Figure 2(a) presents images obtained after the sputter removal of $\approx \frac{1}{2}$ ML (monolayer) of Si, with the substrate held at 400 °C and the ion-beam incident from the [110] direction indicated. Monolayer-deep depressions, or "vacancy islands" have nucleated on all terraces. The depressions are elongated parallel to the dimer rows in the outer atomic layer [Fig. 2(b)]; therefore, at this sputter fluence, depressions occurring in the B domain in Fig. 2(a) may span the entire width of the terrace.

In Fig. 3(a), we observe that sputtering at a higher temperature, 450 °C, does not initially create isolated depressions within a terrace; instead, the surface evolves by step retraction. Therefore, at this temperature a surface vacancy possesses sufficient mobility to reach a step edge, where it can annihilate, causing the retraction of the step edge. At this temperature, depressions appear on the A terrace only after further sputtering [Fig. 3(b)]. Analogously, epitaxial growth at elevated temperatures also suppresses island nucleation and promotes step flow [11].

Examination of Figs. 3(a) and 3(b) reveals that after sputtering, the S_B step has retracted with respect to the S_A, with the consequent depletion of the B domain. In the analogous case of epitaxial growth in the step-flow regime, the S_B step is found to *advance* relative to the S_A, with the consequent *enhancement* of the B domain [12].

Subsequent STM investigations of Si epitaxial growth demonstrated that anisotropic adatom diffusion alone could not have accounted for all the experimental observations, and therefore that an anisotropy in adatom incorporation, favoring attachment at the ends of dimer rows, must be present [8].

Following the analogy with growth [8], we now show that anisotropic vacancy diffusion *alone* cannot account for our observations. Consider the two diffusion directions explicitly [13]. First, if vacancies migrate preferentially parallel to the dimer rows and if vacancy annihilation is isotropic, one would expect the opposite of our result: The A domains would be *depleted* at a substrate temperature where vacancies created on B terraces are sufficiently mobile to reach step edges and annihilate there, but those created on A terraces nucleate vacancy islands. If instead vacancies migrate preferentially perpendicular to dimer rows, then the depletion of B domains might be observed if vacancies created on A terraces are sufficiently mobile to reach step edges and annihilate there, but those created on B terraces nucleate vacancy islands. In fact, we *never* observe vacancy island nucleation on B terraces with the substrate temperature and ion flux that led to Figs. 3(a) and 3(b).

On this basis, we conclude that in the temperature regime corresponding to step retraction, an anisotropy in surface vacancy *annihilation* must be present in order to account for the observed, selective depletion of the B domain following sputtering. Because of the more rapid retraction of the S_B step in Figs. 3(a) and 3(b), we infer that vacancy annihilation takes place preferentially at the ends, rather than the sides, of dimer rows, and that the S_B step is a better vacancy sink than the S_A. Vacancy diffusion might still be anisotropic and may play a role in our observations; however, our findings establish both the existence and the necessity of anisotropic annihilation to explain preferential step retraction. Further study may shed light on the existence and possible role of anisotropic vacancy diffusion by examining the distribution of depressions near good and poor vacancy sinks, such as the monatomic S_B and S_A steps, by analogy with similar experiments reported for growth islands [14].

The anisotropy of vacancy islands in Figs. 2 and 3 is reminiscent of the previously reported anisotropy of *growth* islands, which was attributed to preferred accommodation of *adatoms* at the ends of dimer rows [15,16]. By analogy, preferred annihilation of *vacancies* at the ends of dimer rows would cause *vacancy* islands to grow parallel to the dimer rows in the outer layer, as we observe [Fig. 2(b)]. The shapes and orientation of the observed depressions are therefore consistent with anisotropic vacancy annihilation; further study is required to establish precisely the relative roles of kinetics and energetics in determining the structure of the vacancy islands.

When the surface represented by Fig. 3(b) is annealed briefly at 450 °C, we observe in Fig. 3(c) that the S_B step retreats further, and the B domain is depleted even further than in Fig. 3(b). A natural explanation, consistent with previous diffraction studies of Pt(111) [17] is that, during annealing, atoms detach from step edges and fill in vacancies or depressions in the next lower terrace. These defects serve as sinks for mobile atoms; without such sinks, the preferential detachment of adatoms from S_B steps alone does not lead to a single-domain surface. From Fig. 3(c), we infer that at 450 °C, atoms detach from the S_B steps at a greater rate than from the S_A. This observation is consistent with the previously reported, lower binding energy at an S_B step than at an S_A [8] and the higher predicted stability of an S_A step than an S_B [9]. The novel, single-A-domain surface in Fig. 3(c) is therefore stable under annealing at moderate (≈ 450 °C) temperature. The opposite, single-B-domain surface, which can be created by deposition, is known to be *unstable* to annealing at 450 °C for well-oriented surfaces (offcut $< 4°$) and to revert to a double-domain surface if the substrate is not quenched to room temperature following deposition [8,12]. Therefore, the greater stability of the single-A-domain surface over the single-B-domain surface at 450 °C results from a kinetic consideration, the lower barrier for detachment of Si atoms from the S_B step than the S_A.

We find, however, that annealing the surface shown in Fig. 3(c) at 750 °C for 3 min induces a reversion to the double-domain structure of Fig. 1(a) so the single-A-domain surface is not an equilibrium structure. Its disappearance at higher temperatures is consistent with previous calculations demonstrating that structural considerations, including differing strains inherent in the bonding topologies of the various types of the step edges, make the double-A-step (D_A) energetically unfavorable relative to the three other possible single and double steps which can occur on vicinal Si(100) [9,18,19].

The new, single-A-domain surface is a promising substrate for III/V heteroepitaxy. A double-stepped, single-domain substrate allows the growth of III/V bilayers on Si(100) without antiphase domains [20]. However, only Si substrates of specific misorientation exhibit the single-B-domain structure after annealing; specifically, substrates offcut 4° towards the [110] direction have been used for GaAs/Si growth [21]. Single-B-domain surfaces can also be produced by Si homoepitaxy on better-oriented substrates, but the resulting surface is unstable to domain separation at typical growth temperatures [8,12]. In contrast, the relative kinetic stability of the single-A-domain surface at these temperatures appears to allow the creation of double-stepped, single-domain Si(100) substrates of arbitrary misorientation, and hence domain size.

In summary, we have investigated some of the consequences of anisotropy in the kinetics of mobile surface vacancies on Si(100), which are created during the sputtering of that surface by 225-eV Xe. Preferential annihila-

tion of vacancies at the ends, rather than the sides, of dimer rows leads to the more rapid retraction of the S_B step relative to the S_A step and enables the realization of a new, single-A-domain surface which is not an equilibrium structure because of energetic considerations and is not, to our knowledge, accessible by epitaxial growth alone, but is stabilized at moderately high temperatures ($T \sim 450\,^{\circ}\mathrm{C}$) by kinetic considerations.

The authors are grateful to E. Chason, P. Feibelman, J. Houston, T. Michalske, S. T. Picraux, and B. Poelsema for helpful discussions. This work was supported by BES, Office of Materials Science, under Contract No. DE-AC04-76DP00789.

---

[a]Present address: Materials Science Division, Lawrence Livermore Laboratory, Livermore, CA 94550.

[1] B. Poelsema, L. Verheij, and G. Comsa, Phys. Rev. Lett. **53**, 2500 (1984).
[2] P. Bedrossian, J. E. Houston, E. Chason, J. Y. Tsao, and S. T. Picraux, Phys. Rev. Lett. **67**, 124 (1991).
[3] T. Michely, K. Besocke, and G. Comsa, Surf. Sci. Lett. **230**, L135 (1990).
[4] P. Bedrossian and T. Klitsner, Phys. Rev. B **44**, 13783 (1991).
[5] J. Greene, S. Barnett, J. Sundgren, and A. Rockett, in *Ion Beam Assisted Film Growth*, edited by T. Itoh (Elsevier, Amsterdam, 1989), p. 101.
[6] E. Chason, J. Tsao, K. Horn, S. Picraux, and H. Atwater, J. Vac. Sci. Technol. A **8**, 2507 (1990).
[7] Y. Mo, R. Karotis, B. Swartzentruber, M. Webb, and M. Lagally, J. Vac. Sci. Technol. B **8**, 232 (1990).
[8] A. Hoeven, J. Lenssinck, D. Dijkkamp, E. van Loenen, and J. Dieleman, Phys. Rev. Lett. **63**, 1830 (1989).
[9] D. Chadi, Phys. Rev. Lett. **59**, 1691 (1987).
[10] A. Ishizaka, N. Nakagawa, and Y. Shiraki, in *Proceedings of the Second International Symposium on Molecular Beam Epitaxy and Related Clean Surface Techniques* (Japan Society of Applied Physics, Tokyo, 1982), p. 182.
[11] J. Neave, P. Dobson, B. Joyce, and J. Zhang, Appl. Phys. Lett. **47**, 100 (1985).
[12] T. Sakamoto *et al.*, J. Cryst. Growth **81**, 59 (1987).
[13] S. Stoyanov, J. Cryst. Growth **94**, 751 (1989).
[14] Y. Mo and M. Lagally, Surf. Sci. **248**, 313 (1991).
[15] R. Hamers, U. Köhler, and J. Demuth, Ultramicroscopy **31**, 10 (1989). [STM of Si(100) and (111) epitaxy.]
[16] Y. Mo, B. Swartzentruber, R. Kariotis, M. Webb, and M. Lagally, Phys. Rev. Lett. **63**, 2393 (1989).
[17] B. Poelsema, R. Kunkel, L. Verheij, and G. Comsa, Phys. Rev. B **41**, 11 609 (1990).
[18] O. Alerhand, A. N. Berker, J. Joannopoulos, D. Vanderbilt, R. Hamers, and J. Demuth, Phys. Rev. Lett. **64**, 2401 (1990).
[19] T. Poon, S. Yip, P. Ho, and F. Abraham, Phys. Rev. Lett. **65**, 2161 (1990).
[20] H. Kroemer, in *Heteroepitaxy on Silicon*, edited by J. Fan and J. Poate, MRS Symposia Proceedings No. 67 (Materials Research Society, Pittsburgh, 1986), p. 3.
[21] M. Henzler and J. Clabes, Jpn. J. Appl. Phys. Suppl. **v2**, pt2, 389 (1974).

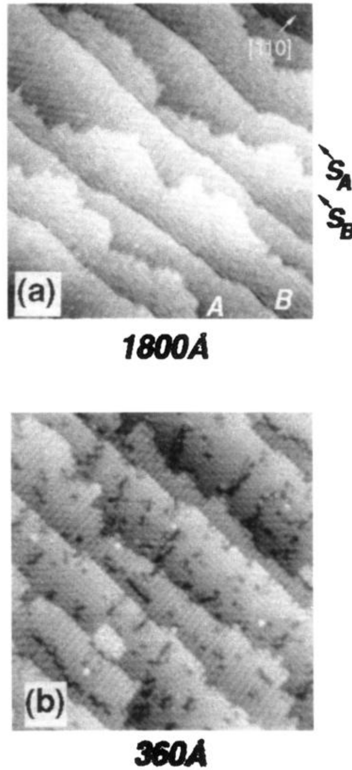

FIG. 1. (a) 1800-Å STM image of the 0.2°-offcut Si(100)-2×1 starting surface for subsequent sputtering. In this and subsequent images, the tunnel current is 0.8 nA and the tip bias +1.8 V, i.e., occupied sample states are imaged. The A and B terraces and the S_A and S_B steps are labeled. (b) Higher-resolution, 360-Å STM image of 1°-offcut Si(100)-2×1, showing the alternating dimer orientation on adjacent terraces. The more offcut sample is shown only in this figure in order to fit several terraces into a higher-resolution image.

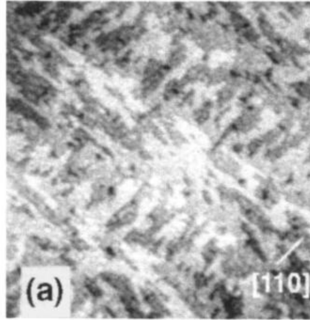

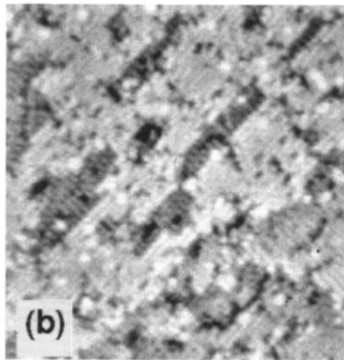

FIG. 2. (a) 1800-Å image of 0.2°-offcut Si(100) following removal of $\approx \frac{1}{2}$ ML by Xe sputtering with the substrate at 400 °C. The ion beam is incident from the [110] direction indicated. (b) 360-Å detail, showing anisotropic, monolayer-deep depressions elongated parallel to the dimer rows of the top layer.

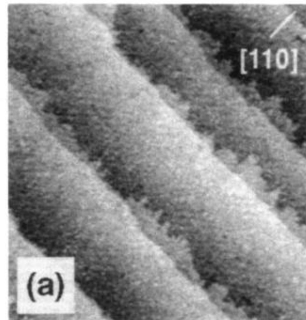

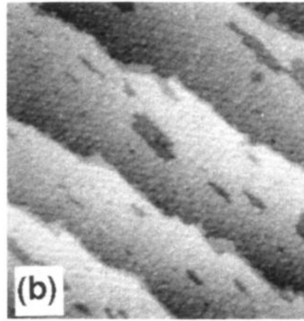

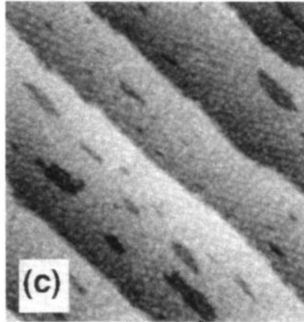

FIG. 3. (a) 1800-Å image following Xe sputtering of $\approx \frac{1}{2}$ ML at 450 °C, showing depletion of the *B* domain. (b) 1800-Å image following Xe sputtering of ≈ 1 ML at 450 °C, showing further depletion of the *B* domain and nucleation of depressions in the *A* domain. (c) 1800-Å image following 6 min of annealing the surface shown in (b) at 450 °C. The *B* domain has virtually disappeared.